



# TECH BRIEFS

NATIONAL AERONAUTICS AND SPACE ADMINISTRATION

-  **Technology Focus**
-  **Electronics/Computers**
-  **Software**
-  **Materials**
-  **Mechanics/Machinery**
-  **Manufacturing**
-  **Bio-Medical**
-  **Physical Sciences**
-  **Information Sciences**
-  **Books and Reports**
-  **Green Design**



# INTRODUCTION

Tech Briefs are short announcements of innovations originating from research and development activities of the National Aeronautics and Space Administration. They emphasize information considered likely to be transferable across industrial, regional, or disciplinary lines and are issued to encourage commercial application.

## Availability of NASA Tech Briefs and TSPs

Requests for individual Tech Briefs or for Technical Support Packages (TSPs) announced herein should be addressed to

### National Technology Transfer Center

Telephone No. (800) 678-6882 or via World Wide Web at [www.nttc.edu](http://www.nttc.edu)

Please reference the control numbers appearing at the end of each Tech Brief. Information on NASA's Innovative Partnerships Program (IPP), its documents, and services is also available at the same facility or on the World Wide Web at <http://www.nasa.gov/offices/ipp/network/index.html>

Innovative Partnerships Offices are located at NASA field centers to provide technology-transfer access to industrial users. Inquiries can be made by contacting NASA field centers listed below.

#### Ames Research Center

Mary Walsh  
(650) 604-1405  
[mary.w.walsh@nasa.gov](mailto:mary.w.walsh@nasa.gov)

#### Dryden Flight Research Center

Yvonne D. Gibbs  
(661) 276-3720  
[yvonne.d.gibbs@nasa.gov](mailto:yvonne.d.gibbs@nasa.gov)

#### Glenn Research Center

Joe Shaw, Acting Chief  
(216) 977-7135  
[robert.j.shaw@nasa.gov](mailto:robert.j.shaw@nasa.gov)

#### Goddard Space Flight Center

Nona Cheeks  
(301) 286-5810  
[nona.k.cheeks@nasa.gov](mailto:nona.k.cheeks@nasa.gov)

#### Jet Propulsion Laboratory

Indrani Graczyk  
(818) 354-2241  
[indrani.graczyk@jpl.nasa.gov](mailto:indrani.graczyk@jpl.nasa.gov)

#### Johnson Space Center

information  
(281) 483-3809  
[jsc.techtran@mail.nasa.gov](mailto:jsc.techtran@mail.nasa.gov)

#### Kennedy Space Center

David R. Makufka  
(321) 867-6227  
[david.r.makufka@nasa.gov](mailto:david.r.makufka@nasa.gov)

#### Langley Research Center

Elizabeth B. Plentovich  
(757) 864-2857  
[elizabeth.b.plentovich@nasa.gov](mailto:elizabeth.b.plentovich@nasa.gov)

#### Marshall Space Flight Center

Jim Dowdy  
(256) 544-7604  
[jim.dowdy@msfc.nasa.gov](mailto:jim.dowdy@msfc.nasa.gov)

#### Stennis Space Center

Ramona Travis  
(228) 688-3832  
[ramona.e.travis@nasa.gov](mailto:ramona.e.travis@nasa.gov)

#### Carl Ray, Program Executive

Small Business Innovation  
Research (SBIR) & Small  
Business Technology  
Transfer (STTR) Programs  
(202) 358-4652  
[carl.g.ray@nasa.gov](mailto:carl.g.ray@nasa.gov)

#### Doug Comstock, Partnerships

Innovation and Commercial  
Space Program Office (formerly IPP)  
(202) 358-2221  
[doug.comstock@nasa.gov](mailto:doug.comstock@nasa.gov)





# TECH BRIEFS

NATIONAL AERONAUTICS AND SPACE ADMINISTRATION



## 5 Technology Focus: Test & Measurement

- 5 Method to Estimate the Dissolved Air Content in Hydraulic Fluid
- 5 Method for Measuring Collimator-Pointing Sensitivity to Temperature Changes
- 6 High-Temperature Thermometer Using Cr-Doped GdAlO<sub>3</sub> Broadband Luminescence
- 6 Metrology Arrangement for Measuring the Positions of Mirrors of a Submillimeter Telescope



## 7 Electronics/Computers

- 7 On-Wafer S-Parameter Measurements in the 325-508-GHz Band
- 7 Reconfigurable Microwave Phase Delay Element for Frequency Reference and Phase-Shifter Applications
- 8 High-Speed Isolation Board for Flight Hardware Testing
- 8 High-Throughput, Adaptive FFT Architecture for FPGA-Based Spaceborne Data Processors



## 11 Software

- 11 3D Orbit Visualization for Earth-Observing Missions
- 11 MaROS: Web Visualization of Mars Orbiting and Landed Assets
- 11 RAPID: Collaborative Commanding and Monitoring of Lunar Assets
- 11 Image Segmentation, Registration, Compression, and Matching
- 12 Image Calibration
- 12 Rapid ISS Power Availability Simulator



## 13 Manufacturing & Prototyping

- 13 A Method of Strengthening Composite/Metal Joints
- 13 Pre-Finishing of SiC for Optical Applications
- 14 Optimization of Indium Bump Morphology for Improved Flip Chip Devices



## 15 Materials & Coatings

- 15 Measuring Moisture Levels in Graphite Epoxy Composite Sandwich Structures
- 15 Marshall Convergent Spray Formulation Improvement for High Temperatures
- 15 Real-Time Deposition Monitor for Ultrathin Conductive Films
- 16 Optimized Li-Ion Electrolytes Containing Triphenyl Phosphate as a Flame-Retardant Additive



## 17 Green Design

- 17 Radiation-Resistant Hybrid Lotus Effect for Achieving Photoelectrocatalytic Self-Cleaning Anticontamination Coatings
- 17 Improved, Low-Stress Economical Submerged Pipeline



## 19 Physical Sciences

- 19 Optical Fiber Array Assemblies for Space Flight on the Lunar Reconnaissance Orbiter
- 20 Local Leak Detection and Health Monitoring of Pressurized Tanks
- 20 Dielectric Covered Planar Antennas at Submillimeter Wavelengths for Terahertz Imaging
- 21 Automated Cryocooler Monitor and Control System
- 21 Broadband Achromatic Phase Shifter for a Nulling Interferometer
- 22 Super Dwarf Wheat for Growth in Confined Spaces
- 22 Fine Guidance Sensing for Coronagraphic Observatories
- 23 Single-Antenna Temperature- and Humidity-Sounding Microwave Receiver
- 23 Multi-Wavelength, Multi-Beam, and Polarization-Sensitive Laser Transmitter for Surface Mapping
- 24 Optical Communications Link to Airborne Transceiver



## 25 Information Sciences

- 25 Ascent Heating Thermal Analysis on Spacecraft Adaptor Fairings
- 25 Entanglement in Self-Supervised Dynamics
- 25 Prioritized LT Codes
- 26 Fast Image Texture Classification Using Decision Trees
- 26 Constraint Embedding Technique for Multibody System Dynamics
- 27 Improved Systematic Pointing Error Model for the DSN Antennas
- 27 Observability and Estimation of Distributed Space Systems via Local Information-Exchange Networks
- 28 More-Accurate Model of Flows in Rocket Injectors
- 28 In-Orbit Instrument-Pointing Calibration Using the Moon as a Target



## 29 Books & Reports

- 29 Reliability of Ceramic Column Grid Array Interconnect Packages Under Extreme Temperatures
- 29 Six Degrees-of-Freedom Ascent Control for Small-Body Touch and Go
- 29 Optical-Path-Difference Linear Mechanism for the Panchromatic Fourier Transform Spectrometer

This document was prepared under the sponsorship of the National Aeronautics and Space Administration. Neither the United States Government nor any person acting on behalf of the United States Government assumes any liability resulting from the use of the information contained in this document, or warrants that such use will be free from privately owned rights.





### Method to Estimate the Dissolved Air Content in Hydraulic Fluid

**A dissolved oxygen meter is used.**

*John H. Glenn Research Center, Cleveland, Ohio*

In order to verify the air content in hydraulic fluid, an instrument was needed to measure the dissolved air content before the fluid was loaded into the system. The instrument also needed to measure the dissolved air content *in situ* and in real time during the de-aeration process. The current methods used to measure the dissolved air content require the fluid to be drawn from the hydraulic system, and additional offline laboratory processing time is involved. During laboratory processing, there is a potential for contamination to occur, especially when sub-saturated fluid is to be analyzed.

A new method measures the amount of dissolved air in hydraulic fluid through the use of a dissolved oxygen meter. The device measures the dissolved air content through an *in situ*,

real-time process that requires no additional offline laboratory processing time. The method utilizes an instrument that measures the partial pressure of oxygen in the hydraulic fluid. By using a standardized calculation procedure that relates the oxygen partial pressure to the volume of dissolved air in solution, the dissolved air content is estimated.

The technique employs luminescent quenching technology to determine the partial pressure of oxygen in the hydraulic fluid. An estimated Henry's law coefficient for oxygen and nitrogen in hydraulic fluid is calculated using a standard method to estimate the solubility of gases in lubricants. The amount of dissolved oxygen in the hydraulic fluid is estimated using the Henry's solubility coefficient and the measured partial

pressure of oxygen in solution. The amount of dissolved nitrogen that is in solution is estimated by assuming that the ratio of dissolved nitrogen to dissolved oxygen is equal to the ratio of the gas solubility of nitrogen to oxygen at atmospheric pressure and temperature. The technique was performed at atmospheric pressure and room temperature. The technique could be theoretically carried out at higher pressures and elevated temperatures.

*This work was done by Daniel M. Hauser of Glenn Research Center. Further information is contained in a TSP (see page 1).*

*Inquiries concerning rights for the commercial use of this invention should be addressed to NASA Glenn Research Center, Innovative Partnerships Office, Attn: Steven Fedor, Mail Stop 4-8, 21000 Brookpark Road, Cleveland, Ohio 44135. Refer to LEW-18621-1.*

### Method for Measuring Collimator-Pointing Sensitivity to Temperature Changes

**A simple, inexpensive, low-tech method is proposed for testing pointing stability versus temperature and other environmental influences.**

*NASA's Jet Propulsion Laboratory, Pasadena, California*

For a variety of applications, it is important to measure the sensitivity of the pointing of a beam emerging from a collimator, as a function of temperature changes. A straightforward method for carrying out this measurement is based on using interferometry for monitoring the changes in beam pointing, which presents its own problems. The added temperature dependence and complexity issues relating to using an interferometer are addressed by not using an interferometer in the first place. Instead, the collimator is made part of an arrangement that uses a minimum number of low-cost, off-the-shelf materials and by using a quad diode to measure changes in beam pointing.

In order to minimize the influence of the test arrangement on the outcome of

the measurement, several steps are taken. The collimator assembly is placed on top of a vertical, 1-m-long, fused silica tube. The quad diode is bonded to a fused silica bar, which, in turn, is bonded to the lower end of the fused silica tube. The lower end of the tube rests on a self-aligning support piece, while the upper end of the tube is kept against two rounded setscrew tips, using a soft rubber string. This ensures that very little stress is applied to the tube as the support structure changes dimensions due to thermal expansion. Light is delivered to the collimator through a bare fiber in order to minimize variable bending torque caused by a randomly relaxing, rigid fiber jacket.

In order to separate the effect of temperature on the collimator assembly

from the effect temperature has on the rest of the setup, multiple measurements are taken with the collimator assembly rotated from measurement to measurement. Laboratory testing, with 1-m spacing between the collimator and the quad diode, has shown that the sensitivity of the arrangement is better than 100 nm rms, over time spans of at least one hour, if the beam path is protected from atmospheric turbulence by a tube. The equivalent sensitivity to detecting changes in pointing angle is 100 nanoradians.

*This work was done by Alex Abramovici, Timothy E. Cox, Randall C. Hein, and Daniel R. MacDonald of Caltech for NASA's Jet Propulsion Laboratory. Further information is contained in a TSP (see page 1). NPO-47529*

---

## High-Temperature Thermometer Using Cr-Doped GdAlO<sub>3</sub> Broadband Luminescence

**Intense high-temperature luminescence enables this thermometer to operate in high thermal radiation backgrounds.**

*John H. Glenn Research Center, Cleveland, Ohio*

A new concept has been developed for a high-temperature luminescence-based optical thermometer that both shows the desired temperature sensitivity in the upper temperature range of present state-of-the-art luminescence thermometers (above 1,300 °C), while maintaining substantial stronger luminescence signal intensity that will allow these optical thermometers to operate in the presence of the high thermal background radiation typical of industrial applications. This objective is attained by using a Cr-doped GdAlO<sub>3</sub> (Cr:GdAlO<sub>3</sub>) sensor with an orthorhombic perovskite structure, resulting in broadband luminescence that remains strong at high temperature due to the favorable electron energy level spacing of Cr:GdAlO<sub>3</sub>.

The Cr:GdAlO<sub>3</sub> temperature (and pressure) sensor can be incorporated into, or applied onto, a component's surface when a non-contact surface temperature measurement is desired, or alternatively, the temperature sensor can be attached to the end of a fiber-optic probe that can then be positioned at the location where the temperature measurement is desired. In the case of the fiber-optic probe, both the

pulsed excitation and the luminescence emission travel through the fiber-optic light guide. In either case, a pulsed light source provides excitation of the luminescence, and the broadband luminescence emission is collected. Real-time temperature measurements are obtained using a least-squares fitting algorithm that determines the luminescence decay time, which has a known temperature dependence established by calibration. Due to the broad absorption and emission bands for Cr:GdAlO<sub>3</sub>, there is considerable flexibility in the choice of excitation wavelength and emission wavelength detection bands.

The strategic choice of the GdAlO<sub>3</sub> host is based on its high crystal field, phase stability, and distorted symmetry at the Cr<sup>3+</sup> occupation sites. The use of the broadband emission for temperature sensing at high temperatures is a key feature of the invention and is novel since broadband luminescence emission normally shows severe thermal quenching. The tightly bound AlO<sub>6</sub> octahedra in GdAlO<sub>3</sub> results in a larger energy barrier to nonradiative decays than in other materials and therefore makes using broadband emission for temperature sensing

possible at high temperatures. This approach results in a substantial increase in temperature capability. For example, the most commonly used Cr-doped crystal used for luminescence-based temperature measurements, ruby, has only been demonstrated up to 600 °C, whereas the Cr:GdAlO<sub>3</sub> optical thermometer under development has already been shown to exhibit useful luminescence up to 1,300 °C. Because GdAlO<sub>3</sub> is non-reactive and is stable in harsh, high-temperature environments, sensors composed of Cr:GdAlO<sub>3</sub> will be very well suited for remote high-temperature measurements in engine or industrial environments where its intense high-temperature luminescence will stand out above significant thermal radiation background levels.

*This work was done by Jeffrey Eldridge of Glenn Research Center and Matthew Chambers. Further information is contained in a TSP (see page 1).*

*Inquiries concerning rights for the commercial use of this invention should be addressed to NASA Glenn Research Center, Innovative Partnerships Office, Attn: Steven Fedor, Mail Stop 4-8, 21000 Brookpark Road, Cleveland, Ohio 44135. Refer to LEW-18614-1.*

---

## Metrology Arrangement for Measuring the Positions of Mirrors of a Submillimeter Telescope

**This system is applicable to any submillimeter radio telescope.**

*NASA's Jet Propulsion Laboratory, Pasadena, California*

The position of the secondary mirror of a submillimeter telescope with respect to the primary mirror needs to be known ≈0.03 mm in three dimensions. At the time of this reporting, no convenient, reasonably priced arrangement that offers this capability exists. The solution proposed here relies on measurement devices developed and deployed for the GeoSAR mission, and later adapted for the ISAT (Innovative Space Based Radar Antenna Technology) demonstration. The measurement arrangement consists of four metrology heads, located on an optical bench, attached to the secondary mirror. Each

metrology head has a dedicated target located at the edge of the primary mirror. One laser beam, launched from the head and returned by the target, is used to measure distance. Another beam, launched from a beacon on the target, is monitored by the metrology head and generates a measurement of the target position in the plane perpendicular to the laser beam.

A 100-MHz modulation is carried by a collimated laser beam. The relevant wavelength is the RF one, 3 m, divided by two, because the light carries it to the target and back. The phase change due to travel to the target and back is meas-

ured by timing the zero-crossing of the RF modulation, using a 100-MHz clock. In order to obtain good resolution, the 100-MHz modulation signal is down-converted to 1 kHz. Then, the phase change corresponding to the round-trip to the target is carried by a 1-kHz signal. Since the 100-MHz clock beats 100,000 times during one period of the 1-kHz signal, the least-significant-bit (LSB) resolution is LSB = 0.015 mm.

*This work was done by Alex Abramovici and Randall K. Bartman of Caltech for NASA's Jet Propulsion Laboratory. Further information is contained in a TSP (see page 1). NPO-47530*



## On-Wafer S-Parameter Measurements in the 325-508-GHz Band

NASA's Jet Propulsion Laboratory, Pasadena, California

New circuits have been designed and fabricated with operating frequencies over 325 GHz. In order to measure S-parameters of these circuits, an extensive process of wafer dicing and packaging, and waveguide transition design, fabrication, and packaging would be required. This is a costly and time-consuming process before the circuit can be tested in waveguide. The new probes and calibration procedures will simplify the testing process.

New on-wafer probes, and a procedure for their calibration, have been developed that allow fast and inexpensive S-parameter

characterization of circuits in the 325-508-GHz frequency band. The on-wafer probes transition from rectangular waveguide to coplanar waveguide probe tips with 40- $\mu\text{m}$  nominal signal-to-ground pin pitch so as to allow for probing circuits on a wafer. The probes with bias tees have been optimized for minimal insertion loss and maximum return loss when placed on 50-ohm structures to allow for calibration. The calibration process has been developed using the Thru-Reflect-Line Agilent algorithm with JPL determined calibration structures and calibration coefficients for the algorithm.

This new test capability is presently unique to JPL. With it, researchers will be able to better develop circuits such as low-noise amplifiers, power amplifiers, multipliers, and mixers for heterodyne receivers in the 325-508-GHz frequency band for remote sensing/spectroscopy.

*This work was done by King Man Fung, Lorene A. Samoska, David M. Pukala, Douglas E. Dawson, Pekka P. Kangaslahti, Todd C. Gaier, and Charles Lawrence of Caltech; Greg Boll of GGB Industries Inc.; and Richard Lai and Xiaobing Mei of NGC for NASA's Jet Propulsion Laboratory. For more information, contact [iaoffice@jpl.nasa.gov](mailto:iaoffice@jpl.nasa.gov). NPO-47575*

## Reconfigurable Microwave Phase Delay Element for Frequency Reference and Phase-Shifter Applications

**This technology can be used in high-resolution phase shifters, frequency references, and oscillators, and in low-temperature sensors.**

Goddard Space Flight Center, Greenbelt, Maryland

A technique was developed to provide a reconfigurable high-precision microwave electrical phase delay for resonators and phase shifters. The invention employs multiple branches of transmission lines with open-ended or ground-ended terminations as configurable bits or digits. This technique minimizes the errors due to limited precision of switching devices. In addition, the proposed linear analytical approach significantly produces a much simpler design than that of other prior inventions at the time of this reporting.

Microwave components such as filters, phase delay elements, or resonators require a method that can accurately adjust their frequency responses. Most tuning techniques offer very wide frequency tuning range; however, it is often difficult and expensive to tune their response in a very narrow operating frequency, especially when the tuning element reaches its minimum discrete step due to fabrication tolerances. The problem becomes worse as the operating frequency is in mm-wave frequency range (>26 GHz).

The electrical tuning sensitivity of a microwave line is dependent on the position of the tuning element with respect to the reference termination. By placing this tuning element away from this reference — with the main transmission line connecting the two elements together — the sensitivity of the tuning element can change significantly. This concept can be used in the system that requires multiple tuning sensitivities. In this case, multiple tuning branches are superimposed in the main transmission line. The proposed invention allows the transmission-line electrical length to be accurately programmed using switching elements that have limited accuracy.

The invention consists of multiple branches of transmission lines connected to discrete switching devices with open-ended terminations. They are used as discrete tuning elements. These elements are connected to the main microwave transmission line and are separated by a well-defined electrical degree spacing. Each branch is pro-

grammed to have different electrical degree sensitivity, such as a combination of discrete steps in each branch, which results in a reflective line with a unique effective phase response. To reduce the number of switching devices, it is desirable to program the devices in binary configuration where each branch represents one bit in the base-2 number system. This invention allows the transmission line electrical length to be tuned precisely with customizable sensitivity based on the known sensitivity of the base tuning circuit. The tuning resolution is dependent on the distance among tuning branches.

The novel feature of this invention is that the phase can be controlled in a very small electrical step of less than 0.5°. The sensitivity of the switching device can be scaled to minimize the errors due to fabrication process. The design technique simplifies the microwave design process. The typical microwave analysis of this device is highly non-linear and is difficult to develop in a closed-form solution. The new inven-

tion uses linear approximation technique that can accurately predict the response. Thus, the overall design process is simplified.

The conceptual model was verified with the circuit simulation, and error due to linear approximation is small and can be compensated by slightly increasing the tuning transmission line

branches by a few percent. The accuracy of the theoretical model is relatively accurate, compared to the circuit model. However, the actual implementation of the invention needs to consider microwave parasitic of the switching devices and discontinuity between any microwave junctions or open-ended terminations. In addition, the absolute

minimum frequency resolution is dependent on the fabrication tolerances and physical implementation of the microwave transmission lines.

*This work was done by Wen-Ting Hsieh, Thomas Stevenson, Christine Jhabvala, Edward Wollack, and Kongpop U-Yen of Goddard Space Flight Center. Further information is contained in a TSP (see page 1). GSC-15704-1*

---

## High-Speed Isolation Board for Flight Hardware Testing

*NASA's Jet Propulsion Laboratory, Pasadena, California*

There is a need to provide a portable and cost-effective galvanic isolation between ground support equipment and flight hardware such that any unforeseen voltage differential between ground and power supplies is eliminated. An interface board was designed for use between the ground support equipment and the flight hardware that electrically isolates all input and output signals and faithfully reproduces them on each side of the interface. It utilizes highly integrated multi-channel isolating devices to minimize size and reduce assembly time.

This single-board solution provides appropriate connector hardware and breakout of required flight signals to individual connectors as needed for vari-

ous ground support equipment. The board utilizes multi-channel integrated circuits that contain transformer coupling, thereby allowing input and output signals to be isolated from one another while still providing high-fidelity reproduction of the signal up to 90 MHz. The board also takes in a single-voltage power supply input from the ground support equipment and in turn provides a transformer-derived isolated voltage supply to power the portion of the circuitry that is electrically connected to the flight hardware.

Prior designs used expensive opto-isolated couplers that were required for each signal to isolate and were time-consuming to assemble. In addition, these earlier designs were bulky and required

a 2U rack-mount enclosure. The new design is smaller than a piece of 8.5×11-in. (≈22×28-mm) paper and can be easily hand-carried where needed.

The flight hardware in question is based on a lineage of existing software-defined radios (SDRs) that utilize a common interface connector with many similar input-output signals present. There are currently four to five variations of this SDR, and more upcoming versions are planned based on the more recent design.

*This work was done by Clifford K. Yamamoto of Caltech, and Richard L. Goodpasture of Mantech SRS Technologies for NASA's Jet Propulsion Laboratory. For more information, contact [iaoffice@jpl.nasa.gov](mailto:iaoffice@jpl.nasa.gov). NPO-47618*

---

## High-Throughput, Adaptive FFT Architecture for FPGA-Based Spaceborne Data Processors

**This architecture can be used in digital circuit design and signal processing, and in onboard instrument data processing.**

*NASA's Jet Propulsion Laboratory, Pasadena, California*

Exponential growth in microelectronics technology such as field-programmable gate arrays (FPGAs) has enabled high-performance spaceborne instruments with increasing onboard data processing capabilities. As a commonly used digital signal processing (DSP) building block, fast Fourier transform (FFT) has been of great interest in onboard data processing applications, which needs to strike a reasonable balance between high-performance (throughput, block size, etc.) and low resource usage (power, silicon footprint, etc.). It is also desirable to be designed so that a single design can be reused and adapted

into instruments with different requirements.

The Multi-Pass Wide Kernel FFT (MPWK-FFT) architecture was developed, in which the high-throughput benefits of the parallel FFT structure and the low resource usage of Singleton's single butterfly method is exploited. The result is a wide-kernel, multi-pass, adaptive FFT architecture.

The 32K-point MPWK-FFT architecture includes 32 radix-2 butterflies, 64 FIFOs to store the real inputs, 64 FIFOs to store the imaginary inputs, complex twiddle factor storage, and FIFO logic to route the outputs to the correct FIFO. The inputs are stored in sequential fash-

ion into the FIFOs, and the outputs of each butterfly are sequentially written first into the even FIFO, then the odd FIFO. Because of the order of the outputs written into the FIFOs, the depth of the even FIFOs, which are 768 each, are 1.5 times larger than the odd FIFOs, which are 512 each. The total memory needed for data storage, assuming that each sample is 36 bits, is 2.95 Mbits. The twiddle factors are stored in internal ROM inside the FPGA for fast access time. The total memory size to store the twiddle factors is 589.9Kbits.

This FFT structure combines the benefits of high throughput from the parallel FFT kernels and low resource usage

from the multi-pass FFT kernels with desired adaptability.

Space instrument missions that need onboard FFT capabilities such as the proposed DESDynI, SWOT (Surface

Water Ocean Topography), and Europa sounding radar missions would greatly benefit from this technology with significant reductions in non-recurring cost and risk.

*This work was done by Kayla Nguyen Kobayashi, Jason X. Zheng, Yutao He, and Biren N. Shah of Caltech for NASA's Jet Propulsion Laboratory. For more information, contact [iaoffice@jpl.nasa.gov](mailto:iaoffice@jpl.nasa.gov). NPO-47531*





## 3D Orbit Visualization for Earth-Observing Missions

This software visualizes orbit paths for the Orbiting Carbon Observatory (OCO), but was designed to be general and applicable to any Earth-observing mission. The software uses the Google Earth user interface to provide a visual mechanism to explore spacecraft orbit paths, ground footprint locations, and local cloud cover conditions. In addition, a drill-down capability allows for users to point and click on a particular observation frame to pop up ancillary information such as data product file names and directory paths, latitude, longitude, time stamp, column-average dry air mole fraction of carbon dioxide, and solar zenith angle.

This software can be integrated with the ground data system for any Earth-observing mission to automatically generate daily orbit path data products in Google Earth KML format. These KML data products can be directly loaded into the Google Earth application for interactive 3D visualization of the orbit paths for each mission day. Each time the application runs, the daily orbit paths are encapsulated in a KML file for each mission day since the last time the application ran. Alternatively, the daily KML for a specified mission day may be generated.

The application automatically extracts the spacecraft position and ground footprint geometry as a function of time from a daily Level 1B data product created and archived by the mission's ground data system software. In addition, ancillary data, such as the column-averaged dry air mole fraction of carbon dioxide and solar zenith angle, are automatically extracted from a Level 2 mission data product. Zoom, pan, and rotate capability are provided through the standard Google Earth interface. Cloud cover is indicated with an image layer from the MODIS (Moderate Resolution Imaging Spectroradiometer) aboard the Aqua satellite, which is automatically retrieved from JPL's OnEarth Web service.

*This work was done by Joseph C. Jacob, Lucian Plesea, Brian G. Chafin, and Barry H. Weiss of Caltech for NASA's Jet Propulsion Laboratory. Further information is contained in a TSP (see page 1).*

*This software is available for commercial licensing. Please contact Daniel Broderick of*

*the California Institute of Technology at danielb@caltech.edu. Refer to NPO-47316.*

## MaROS: Web Visualization of Mars Orbiting and Landed Assets

Mars Relay operations currently involve several e-mails and phone calls between lander and orbiter teams in order to settle on an agreed time for performing a communication pass between the landed asset (i.e. rover or lander) and orbiter, then back to Earth. This new application aims to reduce this complexity by presenting a visualization of the overpass time ranges and elevation angle, as well as other information. The user is able to select a specific overflight opportunity to receive further information about that particular pass.

This software presents a unified view of the potential communication passes available between orbiting and landed assets on Mars. Each asset is presented to the user in a graphical view showing overpass opportunities, elevation angle, requested and acknowledged communication windows, forward and back latencies, warnings, conflicts, relative planetary times, ACE Schedules, and DSN information.

This software is unique in that it is the first of its kind to visually display the information regarding communication opportunities between landed and orbiting Mars assets. The software is written using ActionScript/FLEX, a Web language, meaning that this information may be accessed over the Internet from anywhere in the world.

*This work was done by Michael N. Wallick, Daniel A. Allard, Roy E. Gladden, and Franklin H. Hy of Caltech for NASA's Jet Propulsion Laboratory. For more information, contact iaoffice@jpl.nasa.gov.*

*This software is available for commercial licensing. Please contact Daniel Broderick of the California Institute of Technology at danielb@caltech.edu. Refer to NPO-47413.*

## RAPID: Collaborative Commanding and Monitoring of Lunar Assets

RAPID (Robot Application Programming Interface Delegate) software utilizes highly robust technology to facilitate commanding and monitoring of lunar as-

sets. RAPID provides the ability for inter-center communication, since these assets are developed in multiple NASA centers.

RAPID is targeted at the task of lunar operations; specifically, operations that deal with robotic assets, cranes, and astronaut spacesuits, often developed at different NASA centers. RAPID allows for a uniform way to command and monitor these assets. Commands can be issued to take images, and monitoring is done via telemetry data from the asset.

There are two unique features to RAPID: First, it allows any operator from any NASA center to control any NASA lunar asset, regardless of location. Second, by abstracting the native language for specific assets to a common set of messages, an operator may control and monitor any NASA lunar asset by being trained only on the use of RAPID, rather than the specific asset.

RAPID is easier to use and more powerful than its predecessor, the Astronaut Interface Device (AID). Utilizing the new robust middleware, DDS (Data Distribution System), developing in RAPID has increased significantly over the old middleware. The API is built upon the Java Eclipse Platform, which combined with DDS, provides platform-independent software architecture, simplifying development of RAPID components. As RAPID continues to evolve and new messages are being designed and implemented, operators for future lunar missions will have a rich environment for commanding and monitoring assets.

*This work was done by Recaredo J. Torres, David S. Mittman, Mark W. Powell, Jeffrey S. Norris, Joseph C. Joswig, Thomas M. Crockett, Lucy Abramyan, Khawaja S. Shams, and Michael N. Wallick of Caltech; Mark Allan of Ames Research Center; and Robert Hirsh of Johnson Space Center for NASA's Jet Propulsion Laboratory. For more information, contact iaoffice@jpl.nasa.gov.*

*This software is available for commercial licensing. Please contact Daniel Broderick of the California Institute of Technology at danielb@caltech.edu. Refer to NPO-46332.*

## Image Segmentation, Registration, Compression, and Matching

A novel computational framework was developed of a 2D affine invariant matching exploiting a parameter space. Named

as affine invariant parameter space (AIPS), the technique can be applied to many image-processing and computer-vision problems, including image registration, template matching, and object tracking from image sequence.

The AIPS is formed by the parameters in an affine combination of a set of feature points in the image plane. In cases where the entire image can be assumed to have undergone a single affine transformation, the new AIPS match metric and matching framework becomes very effective (compared with the state-of-the-art methods at the time of this reporting). No knowledge about scaling or any other transformation parameters need to be known *a priori* to apply the AIPS framework.

An automated suite of software tools has been created to provide accurate image segmentation (for data cleaning) and high-quality 2D image and 3D surface registration (for fusing multi-resolution terrain, image, and map data). These tools are capable of supporting existing GIS toolkits already in the marketplace, and will also be usable in a stand-alone fashion. The toolkit applies novel algorithmic approaches for image segmentation, feature extraction, and registration of 2D imagery and 3D surface data, which supports first-pass, batched, fully automatic feature extraction (for segmentation), and registration.

A hierarchical and adaptive approach is taken for achieving automatic feature extraction, segmentation, and registration. Surface registration is the process of aligning two (or more) data sets to a common coordinate system, during which the transformation between their different coordinate systems is determined.

Also developed here are a novel, volumetric surface modeling and compression technique that provide both quality-guaranteed mesh surface approximations and compaction of the model sizes by efficiently coding the geometry and connectivity/topology components of the generated models. The highly efficient triangular mesh compression compacts the connectivity information at the rate of 1.5–4 bits per

vertex (on average for triangle meshes), while reducing the 3D geometry by 40–50 percent.

Finally, taking into consideration the characteristics of 3D terrain data, and using the innovative, regularized binary decomposition mesh modeling, a multi-stage, pattern-drive modeling, and compression technique has been developed to provide an effective framework for compressing digital elevation model (DEM) surfaces, high-resolution aerial imagery, and other types of NASA data.

*This work was done by Jacob Yadegar, Hai Wei, Joseph Yadegar, Nilanjan Ray, and Sakina Zabuwala of UtopiaCompression Corp. for Stennis Space Center.*

*Inquiries concerning rights for its commercial use should be addressed to:*

*Utopia Compression*

*11150 W. Olympic Blvd Suite 1020*

*Los Angeles, CA 90064-1822*

*Telephone No. (310) 473-1500*

*E-mail: jacob@utopiacompression.com*

*Refer to SSC-00304/5/6/7, volume and number of this NASA Tech Briefs issue, and the page number.*

---

## Image Calibration

Calibrate\_Image calibrates images obtained from focal plane arrays so that the output image more accurately represents the observed scene. The function takes as input a degraded image along with a flat field image and a dark frame image produced by the focal plane array and outputs a corrected image. The three most prominent sources of image degradation are corrected for: dark current accumulation, gain non-uniformity across the focal plane array, and hot and/or dead pixels in the array. In the corrected output image the dark current is subtracted, the gain variation is equalized, and values for hot and dead pixels are estimated, using bicubic interpolation techniques.

*This work was done by Christopher S. Peay and David M. Palacios of Caltech for NASA's Jet Propulsion Laboratory. For more information, contact iaoffice@jpl.nasa.gov.*

*The software used in this innovation is available for commercial licensing. Please con-*

*tact Daniel Broderick of the California Institute of Technology at danielb@caltech.edu. Refer to NPO-47191.*

---

## Rapid ISS Power Availability Simulator

The ISS (International Space Station) Power Resource Officers (PROs) needed a tool to automate the calculation of thousands of ISS power availability simulations used to generate power constraint matrices. Each matrix contains 864 cells, and each cell represents a single power simulation that must be run. The tools available to the flight controllers were very operator intensive and not conducive to rapidly running the thousands of simulations necessary to generate the power constraint data.

SOLAR is a Java-based tool that leverages commercial-off-the-shelf software (Satellite Toolkit) and an existing in-house ISS EPS model (SPEED) to rapidly perform thousands of power availability simulations. SOLAR has a very modular architecture and consists of a series of plug-ins that are loosely coupled. The modular architecture of the software allows for the easy replacement of the ISS power system model simulator, re-use of the Satellite Toolkit integration code, and separation of the user interface from the core logic.

Satellite Toolkit (STK) is used to generate ISS eclipse and insulation times, solar beta angle, position of the solar arrays over time, and the amount of shadowing on the solar arrays, which is then provided to SPEED to calculate power generation forecasts.

The power planning turn-around time is reduced from three months to two weeks (83-percent decrease) using SOLAR, and the amount of PRO power planning support effort is reduced by an estimated 30 percent.

*This work was done by Nicholas Downing of United Space Alliance for Johnson Space Center. For further information, contact the JSC Innovation Partnerships Office at (281) 483-3809. MSC-24623-1*



## A Method of Strengthening Composite/Metal Joints

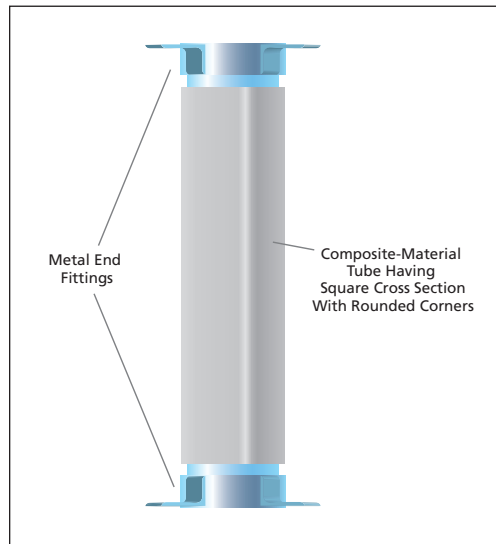
**This method is a less-expensive, easier alternative to a prior method.**

*Goddard Space Flight Center, Greenbelt, Maryland*

The term “tape setback method” denotes a method of designing and fabricating bonded joints between (1) box beams or other structural members made of laminated composite (matrix/fiber) materials and (2) metal end fittings used to fasten these structural members to other structural members. The basic idea of the tape setback method is to mask the bonded interface between the metallic end fitting and composite member such that the bond does not extend out to the free edges of the composite member.

The purpose served by the tape setback method is to strengthen the joints by decoupling stress concentrations from edge defects, which can cause premature failures. A related prior method that serves a similar purpose, involving the use of tapered adherends at the joints, can be too difficult and costly to be acceptable in some applications. The tape setback method offers an easier, less costly alternative. The structural

members to which the method was originally applied were box beams in the form of composite tubes having flat faces with rounded corners. The end



A Composite-Material Box Beam with metal end fittings, shown here not to scale, is representative of the structural members on which the tape setback method was demonstrated.

fittings were plugs made of a low-thermal-expansion nickel/iron alloy (see figure). In computational-simulation studies of tensile and compressive loading of members without tape setback, stresses were found to be concentrated at the free end edges of the composite tubes, and inspection of members that had been subjected to real tension and compression tests showed that cracks started at the free end edges.

As applied to these members, the tape setback method makes them less vulnerable to initiation of failure at edge defects produced during fabrication. In real tension tests of comparable members without and with tape setback, the average mean tensile strength of the members with tape setback was found to be 1.9 times that of the members without tape setback.

*This work was done by Daniel L. Polis of Goddard Space Flight Center. Further information is contained in a TSP (see page 1). GSC-15506-1*

## Pre-Finishing of SiC for Optical Applications

*Goddard Space Flight Center, Greenbelt, Maryland*

A method is based on two unique processing steps that are both based on deterministic machining processes using a single-point diamond turning (SPDT) machine. In the first step, a high-MRR (material removal rate) process is used to machine the part within several microns of the final geometry. In the second step, a low-MRR process is used to machine the part to near optical quality using a novel ductile regime machining (DRM) process.

DRM is a deterministic machining process associated with conditions under high hydrostatic pressures and very small depths of cut. Under such conditions, using high negative-rake angle cutting tools, the high-pressure region near the

tool corresponds to a plastic zone, where even a brittle material will behave in a ductile manner.

In the high-MRR processing step, the objective is to remove material with a sufficiently high rate such that the process is economical, without inducing large-scale subsurface damage. A laser-assisted machining approach was evaluated whereby a CO<sub>2</sub> laser was focused in advance of the cutting tool. While CVD (chemical vapor deposition) SiC was successfully machined with this approach, the cutting forces were substantially higher than cuts at room temperature under the same machining conditions. During the experiments, the expansion of the part and the tool due to the heating was carefully accounted for. The

higher cutting forces are most likely due to a small reduction in the shear strength of the material compared with a larger increase in friction forces due to the thermal softening effect.

The key advantage is that the hybrid machine approach has the potential to achieve optical quality without the need for a separate optical finishing step. Also, this method is scalable, so one can easily progress from machining 50-mm-diameter samples to the 250-mm-diameter mirror that NASA desires.

*This work was done by Jay Rozzi, Odile Clavier, and John Gagne of Creare, Inc. for Goddard Space Flight Center. Further information is contained in a TSP (see page 1). GSC-15663-1*

## Optimization of Indium Bump Morphology for Improved Flip Chip Devices

**Flip chips have applications in cell phones and other small electronic devices.**

*NASA's Jet Propulsion Laboratory, Pasadena, California*

Flip-chip hybridization, also known as bump bonding, is a packaging technique for microelectronic devices that directly connects an active element or detector to a substrate readout face-to-face, eliminating the need for wire bonding. In order to make conductive links between the two parts, a solder material is used between the bond pads on each side. Solder bumps, composed of indium metal, are typically deposited by thermal evaporation onto the active regions of the device and substrate. While indium bump technology has been a part of the electronic interconnect process field for many years and has been extensively employed in the infrared imager industry, obtaining a reliable, high-yield process for high-density patterns of bumps can be quite difficult.

Under the right conditions, a moderate hydrogen plasma exposure can raise the temperature of the indium bump to the point where it can flow. This flow can result in a desirable shape where indium will efficiently wet the metal contact pad to provide good electrical contact to the underlying readout or imager circuit. However, it is extremely important to carefully control this process as the intensity of the hydrogen plasma treat-

ment dramatically affects the indium bump morphology.

To ensure the fine-tuning of this reflow process, it is necessary to have real-time feedback on the status of the bumps. With an appropriately placed viewport in a plasma chamber, one can image a small field (a square of approximately 5 millimeters on each side) of the bumps (10-20 microns in size) during the hydrogen plasma reflow process. By monitoring the shape of the bumps in real time using a video camera mounted to a telescoping 12× magnifying zoom lens and associated optical elements, an engineer can precisely determine when the reflow of the bumps has occurred, and can shut off the plasma before evaporation or de-wetting takes place.

This reflow process has been demonstrated to yield streak-free imagers, and repair misaligned or otherwise damaged indium bumps. It has also been demonstrated to yield non-resistive indium bump contacts in hybridized imagers having large arrays of information processing contacts. Without the reflow process, some 15 percent of the indium contacts were affected by unwanted resistance from oxidized or otherwise damaged indium bumps.

This technology has broad applications to all types of hybridized sensors and is not limited to space applications. Bump-bonding technology, in general, is useful in applications where a reduction in the packaging size of a completed device is advantageous. Because wire bonds are unnecessary in bump-bonded devices, the flip chips can sit directly on their corresponding circuit boards, resulting in a reduction of carrier area and height.

*This work was done by Todd J. Jones, Shouleh Nikzad, Thomas J. Cunningham, Edward Blazejewski, Matthew R. Dickie, Michael E. Hoenk, and Harold F. Greer of Caltech for NASA's Jet Propulsion Laboratory. Further information is contained in a TSP (see page 1).*

*In accordance with Public Law 96-517, the contractor has elected to retain title to this invention. Inquiries concerning rights for its commercial use should be addressed to:*

*Innovative Technology Assets Management  
JPL*

*Mail Stop 202-233*

*4800 Oak Grove Drive*

*Pasadena, CA 91109-8099*

*E-mail: [iaoffice@jpl.nasa.gov](mailto:iaoffice@jpl.nasa.gov)*

*Refer to NPO-47422, volume and number of this NASA Tech Briefs issue, and the page number.*



## Measuring Moisture Levels in Graphite Epoxy Composite Sandwich Structures

*John F. Kennedy Space Center, Florida*

Graphite epoxy composite (GEC) materials are used in the construction of rocket fairings, nose cones, interstage adapters, and heat shields due to their high strength and light weight. However, they absorb moisture depending on the environmental conditions they are exposed to prior to launch. Too much moisture absorption can become a problem when temperature and pressure changes experienced during launch cause the water to vaporize. The rapid state change of the water can result in structural failure of the material. In addition, heat and moisture combine to weaken GEC structures. Diffusion models that predict the

total accumulated moisture content based on the environmental conditions are one accepted method of determining if the material strength has been reduced to an unacceptable level. However, there currently doesn't exist any field measurement technique to estimate the actual moisture content of a composite structure.

A multi-layer diffusion model was constructed with Mathematica to predict moisture absorption and desorption from the GEC sandwich structure. This model is used in conjunction with relative humidity/temperature sensors both on the inside and outside of the material to determine the moisture levels in the

structure. Because the core materials have much higher diffusivity than the face sheets, a single relative humidity measurement will accurately reflect the moisture levels in the core. When combined with an external relative humidity measurement, the model can be used to determine the moisture levels in the face sheets. Since diffusion is temperature-dependent, the temperature measurements are used to determine the diffusivity of the face sheets for the model computations.

*This work was done by Mark Nurge, Robert Youngquist, and Stanley Starr of Kennedy Space Center. Further information is contained in a TSP (see page 1). KSC-13499*

## Marshall Convergent Spray Formulation Improvement for High Temperatures

*Lyndon B. Johnson Space Center, Houston, Texas*

The Marshall Convergent Coating-1 (MCC-1) formulation was produced in the 1990s, and uses a standard bisphenol A epoxy resin system with a triamine accelerator. With the increasing heat rates forecast for the next generation of vehicles, higher-temperature sprayable coatings are needed.

This work substitutes the low-temperature epoxy resins used in the MCC-1 coating with epoxy phenolic, epoxy novalac, or resorcinolic resins (higher carbon con-

tent), which will produce a higher char yield upon exposure to high heat and increased glass transition temperature.

High-temperature filler materials, such as granular cork and glass ecospheres, are also incorporated as part of the convergent spray process, but other sacrificial (ablativ) materials are possible. In addition, the use of polyhedral oligomeric silsesquioxanes (POSS) nanoparticle hybrids will increase both reinforcement aspects and contribute to creating a

tougher silicious char, which will reduce recession at higher heat rates. Use of expanding epoxy resin (lightweight MCC) systems are also useful in that they reduce system weight, have greater insulative properties, and a decrease in application times can be realized.

*This work was done by Jack Scarpa and Chat Patterson of United Space Alliance for Johnson Space Center. For further information, contact the JSC Innovation Partnerships Office at (281) 483-3809. MSC-24644-1*

## Real-Time Deposition Monitor for Ultrathin Conductive Films

*John H. Glenn Research Center, Cleveland, Ohio*

A device has been developed that can be used for the real-time monitoring of ultrathin (2 Å or more) conductive films. The device responds in less than two microseconds, and can be used to monitor film depositions up to about 60 Å thick. Actual thickness

monitoring capability will vary based on properties of the film being deposited. This is a single-use device, which, due to the very low device cost, can be disposable.

Conventional quartz/crystal microbalance devices have proven inadequate to

monitor the thickness of Pd films during deposition of ultrathin films for hydrogen sensor devices. When the deposited film is less than 100 Å, the QCM measurements are inadequate to allow monitoring of the ultrathin films being developed. Thus, an improved, high-

sensitivity, real-time deposition monitor was needed to continue Pd film deposition development.

The new deposition monitor utilizes a surface acoustic wave (SAW) device in a differential delay-line configuration to produce both a reference response and a response for the portion of the device on which the film is being deposited. Both responses are monitored simultaneously during deposition. The reference response remains unchanged, while the attenuation of the sensing path (where the film is being deposited) varies as the film thickness increases.

This device utilizes the fact that on high-coupling piezoelectric substrates,

the attenuation of an SAW undergoes a transition from low to very high, and back to low as the conductivity of a film on the device surface goes from non-conductive to highly conductive. Thus, the sensing path response starts with a low insertion loss, and as a conductive film is deposited, the film conductivity increases, causing the device insertion loss to increase dramatically (by up to 80 dB or more), and then with continued film thickness increases (and the corresponding conductivity increases), the device insertion loss goes back down to the low level at which it started. This provides a continuous, real-time monitoring of film deposition. For use with

different films, the device would need to be calibrated to provide an understanding of how film thickness is related to film conductivity, as the device is responding primarily to conductivity effects (and not to mass loading effects) in this ultrathin film regime.

*This work was done by Jacqueline Hines of Applied Sensor Research & Development Corp. for Glenn Research Center. Further information is contained in a TSP (see page 1).*

*Inquiries concerning rights for the commercial use of this invention should be addressed to NASA Glenn Research Center, Innovative Partnerships Office, Attn: Steven Fedor, Mail Stop 4-8, 21000 Brookpark Road, Cleveland, Ohio 44135. Refer to LEW-18651-1.*

## Optimized Li-Ion Electrolytes Containing Triphenyl Phosphate as a Flame-Retardant Additive

**This technology is applicable to portable electronics, electric vehicles, and other applications requiring safety and performance over a wide temperature range.**

*NASA's Jet Propulsion Laboratory, Pasadena, California*

A number of future NASA missions involving the exploration of the Moon and Mars will be "human-rated" and thus require high-specific-energy rechargeable batteries that possess enhanced safety characteristics. Given that Li-ion technology is the most viable rechargeable energy storage device for near-term applications, effort has been devoted to improving the safety characteristics of this system. There is also a strong desire to develop Li-ion batteries with improved safety characteristics for terrestrial applications, most notably for hybrid electric vehicle (HEV) and plug-in hybrid electric vehicle (PHEV) automotive applications. Therefore, extensive effort has been devoted recently to developing non-flammable electrolytes to reduce the flammability of the cells/battery.

A number of electrolyte formulations have been developed, including systems that (1) incorporate greater concentrations of the flame-retardant additive (FRA); (2) use di-2,2,2-trifluoroethyl carbonate (DTFEC) as a co-solvent; (3) use 2,2,2-trifluoroethyl methyl carbonate

(TFEMC); (4) use mono-fluoroethylene carbonate (FEC) as a co-solvent and/or a replacement for ethylene carbonate in the electrolyte mixture; and (5) utilize vinylene carbonate as a "SEI promoting" electrolyte additive, to build on the favorable results previously obtained.

To extend the family of electrolytes developed under previous work, a number of additional electrolyte formulations containing FRAs, most notably triphenyl phosphate (TPP), were investigated and demonstrated in experimental MCMB (mesocarbon microbeads) carbon-LiNi<sub>0.8</sub>Co<sub>0.2</sub>O<sub>2</sub> cells. The use of higher concentrations of the FRA is known to reduce the flammability of the electrolyte solution, thus, a concentration range was investigated (i.e., 5 to 20 percent by volume). The desired concentration of the FRA is the highest amount tolerable without adversely affecting the performance in terms of reversibility, ability to operate over a wide temperature range, and the discharge rate capability.

The use of fluorinated carbonates, much in the same manner as the incor-

poration of fluorinated ester-based solvents, was employed to reduce the inherent flammability of mixtures. Thus, electrolyte formulations that embody both approaches are anticipated to have much lower flammability, resulting in enhanced safety.

*This work was done by Marshall C. Smart and Ratnakumar V. Bugga of Caltech and G. K. Surya Prakash and Frederick C. Krause of the University of Southern California for NASA's Jet Propulsion Laboratory. Further information is contained in a TSP (see page 1).*

*In accordance with Public Law 96-517, the contractor has elected to retain title to this invention. Inquiries concerning rights for its commercial use should be addressed to:*

*Innovative Technology Assets Management  
JPL*

*Mail Stop 202-233*

*4800 Oak Grove Drive*

*Pasadena, CA 91109-8099*

*E-mail: iaoffice@jpl.nasa.gov*

*Refer to NPO-47465, volume and number of this NASA Tech Briefs issue, and the page number.*

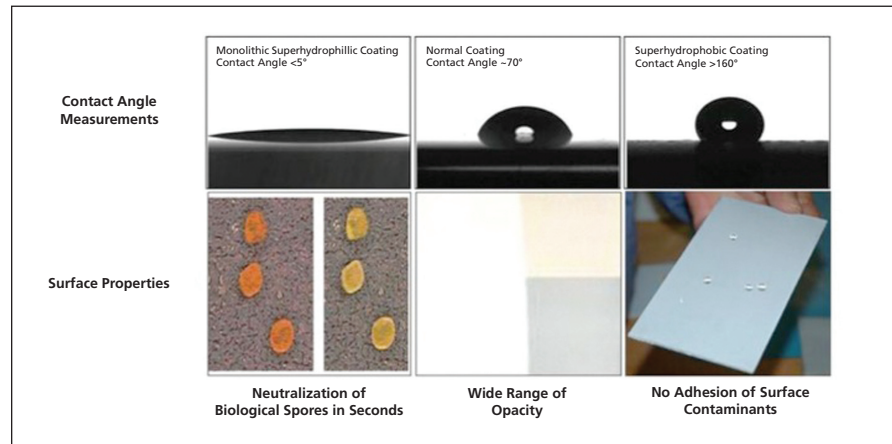


## **Radiation-Resistant Hybrid Lotus Effect for Achieving Photoelectrocatalytic Self-Cleaning Anticontamination Coatings** Initial results are promising.

*Goddard Space Flight Center, Greenbelt, Maryland*

An experiment involving radiation-resistant hydrophobic coatings is planned for space exposure and experimental testing on the International Space Station (ISS) in 2011. The Lotus biocide coatings are designed for supporting space exploration missions. This innovation is an antibacterial, anti-contamination, and self-cleaning coating that uses nano-sized semiconductor semimetal oxides to neutralize biological pathogens and toxic chemicals, as well as to mitigate dust accumulation (see figure).

The Lotus biocide coating is thin (approximately microns thick), lightweight, and the biocide properties will not degrade with time or exposure to biological or chemical agents. The biocide is stimulated chemically (stoichiometric reaction) through exposure to light (photocatalysis), or by an applied electric field (electrocatalysis). The hydrophobic coating samples underwent preliminary high-energy proton and alpha-ray (helium ion) irradiations at the Lawrence Berkeley National Laboratory 88" cyclotron and demonstrated excellent radiation resistance for a portion



The first row of photos shows the **Behavior of a Water Droplet's Contact Angle** on superhydrophillic, normal, and superhydrophobic coated surfaces. Little or no change in the contact angles was observed following irradiation of the coatings by gamma-rays and high-energy protons. The bottom row of photos illustrates that radiation-resistant self-cleaning coatings also offer the potential to reduce terrestrial and extraterrestrial cleaning requirements on surfaces while providing biocidal and spore-repellent features.

of the Galactic Cosmic Ray (GRC) and Solar Proton spectrum. The samples will undergo additional post-flight studies when returned to Earth to affirm further the radiation resistance properties of the space exposed coatings.

*This work was conducted by Edward W. Taylor of International Photonics Consultants and Ronald G. Pirich of Northrop Grumman for Goddard Space Flight Center. Further information is contained in a TSP (see page 1). GSC 16117-1*

## **Improved, Low-Stress Economical Submerged Pipeline**

**This technology can safely transport large quantities of fresh water, oil, and natural gas underwater for long distances.**

*NASA's Jet Propulsion Laboratory, Pasadena, California*

A preliminary study has shown that the use of a high-strength composite fiber cloth material may greatly reduce fabrication and deployment costs of a subsea offshore pipeline. The problem is to develop an inexpensive submerged pipeline that can safely and economically transport large quantities of fresh water, oil, and natural gas underwater for long distances. Above-water pipelines are often not feasible due to safety, cost, and environmental problems, and present, fixed-wall, sub-

merged pipelines are often very expensive.

The solution is to have a submerged, compliant-walled tube that when filled, is lighter than the surrounding medium. Some examples include compliant tubes for transporting fresh water under the ocean, for transporting crude oil underneath salt or fresh water, and for transporting high-pressure natural gas from offshore to onshore.

In each case, the fluid transported is lighter than its surrounding fluid, and

thus the flexible tube will tend to float. The tube should be ballasted to the ocean floor so as to limit the motion of the tube in the horizontal and vertical directions. The tube should be placed below 100-m depth to minimize biofouling and turbulence from surface storms. The tube may also have periodic pumps to maintain flow without over-pressurizing, or it can have a single pump at the beginning. The tube may have periodic valves that allow sections of the tube to be repaired or maintained. Some exam-

ples of tube materials that may be particularly suited for these applications are non-porous composite tubes made of high-performance fibers such as Kevlar, Spectra, PBO, Aramid, carbon fibers, or high-strength glass.

Above-ground pipes for transporting water, oil, and natural gas have typically been fabricated from fiber-reinforced

plastic or from more costly high-strength steel. Also, previous suggested subsea pipeline designs have only included heavy fixed-wall pipes that can be very expensive initially, and can be difficult and expensive to deploy for long distances. A much less expensive Kevlar pipeline can be coiled up on a ship's deck and deployed in the water as the

ship moves. Support ships can be used to drop sand into conduits below the uninflated tube, so that the tube remains in place when more buoyant fresh water later fills the tubes.

*This work was done by Jack A. Jones and Yi Chao of Caltech for NASA's Jet Propulsion Laboratory. Further information is contained in a TSP (see page 1). NPO-47455*



## Optical Fiber Array Assemblies for Space Flight on the Lunar Reconnaissance Orbiter

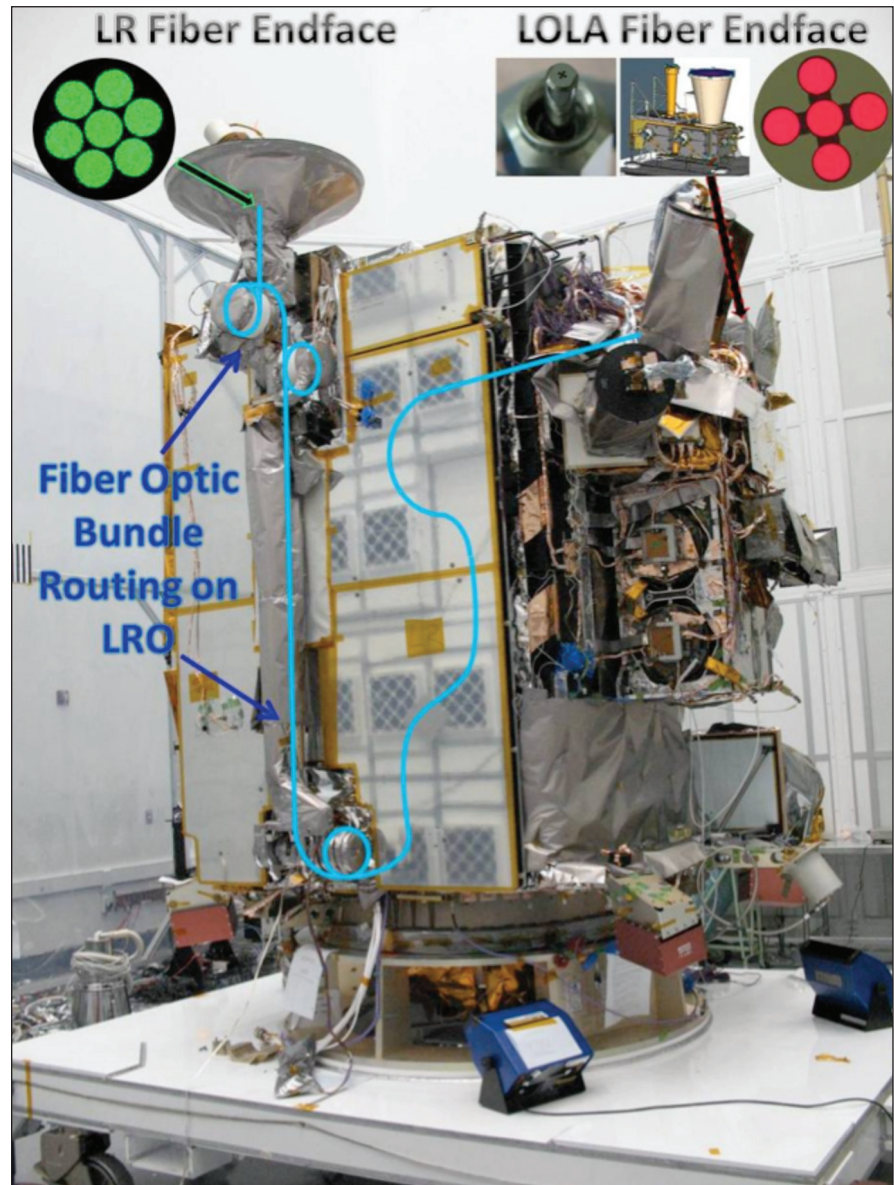
Optical fiber array bundle assemblies are used in a high performance space flight application.

*Goddard Space Flight Center, Greenbelt, Maryland*

Custom fiber optic bundle array assemblies developed by the Photonics Group at NASA Goddard Space Flight Center were an enabling technology for both the Lunar Orbiter Laser Altimeter (LOLA) and the Laser Ranging (LR) Investigation on the Lunar Reconnaissance Orbiter (LRO) currently in operation. The unique assembly array designs provided considerable decrease in size and weight and met stringent system level requirements.

This is the first time optical fiber array bundle assemblies were used in a high performance space flight application. This innovation was achieved using customized Diamond Switzerland AVIM optical connectors. For LOLA, a five fiber array was developed for the receiver telescope to maintain precise alignment for each of the 200/220 micron optical fibers collecting 1,064 nm wavelength light being reflected back from the moon. The array splits to five separate detectors replacing the need for multiple telescopes. An image illustration of the LOLA instrument can be found at the top of the figure.

For the laser ranging, a seven-optical-fiber array of 400/440 micron fibers was developed to transmit light from behind the LR receiver telescope located on the end of the high gain antenna system (HGAS). The bundle was routed across two moving gimbals, down the HGAS boom arm, over a deployable mandrel and across the spacecraft to a detector on the LOLA instrument. The routing of the optical fiber bundle and its end locations is identified in the figure. The Laser Ranging array and bundle is currently accepting light at a wavelength of 532 nm sent to the moon from laser stations at Greenbelt MD and other stations around the world to gather precision ranging information from the Earth to the LRO spacecraft. The LR bundle assembly is capable of withstanding temperatures down to  $-55^{\circ}\text{C}$  at the connectors, and 20,000 mechanical gimbal cycles at temperatures as cold as  $-20^{\circ}\text{C}$  along the



The integrated LRO showing the optical fiber bundle routing, the locations of the array assembly connectors, and the location of the LOLA instrument. Also pictured are 400X magnification images of the optical fiber array endfaces at the approximate locations in which they are integrated.

length of the seven-fiber bundle (that is packaged into the gimbals). The total bundle assembly is 10 meters long with two interconnections requiring precise clocking of the seven-fiber array pattern.

*This work was done by Melanie Ott and Adam Matuszeski of Goddard Space Flight Center. Further information is contained in a TSP (see page 1). GSC-15930-1*

## Local Leak Detection and Health Monitoring of Pressurized Tanks

Marshall Space Flight Center, Alabama

An optical gas-detection sensor safely monitors pressurized systems (such as cryogenic tanks) and distribution systems for leaks. This sensor system is a fiber-coupled, solid optical body interferometer that allows for the miniaturized sensing element of the device to be placed in the smallest of recesses, and measures a wide range of gas species and densities (leaks). The deflection of the fringe pattern is detected and recorded to yield the time-varying gas density in the gap. This technology can be used by manufacturers or storage fa-

cilities with toxic, hazardous, or explosive gases.

The approach is to monitor the change in the index of refraction associated with low-level gas leaks into a vacuum environment. The completion of this work will provide NASA with an enabling capability to detect gas system leaks in space, and to verify that pressurized systems are in a safe (i.e. non-leaking) condition during manned docking and transit operations.

By recording the output of the sensor, a time-history of the leak can be constructed to indicate its severity. Project

risk is mitigated by having several interferometric geometries and detection techniques available, each potentially leveraging hardware and lessons learned to enhance detectability.

*This work was done by Kurt Polzin and William Witherow of Marshall Space Flight Center; Valentin Korman formerly of Madison Research Corp; John Sinko of Kratos Defense; and Adam Hendrickson of the U.S. Army. For more information, contact Sammy Nabors, MSFC Commercialization Assistance Lead, at [sammy.a.nabors@nasa.gov](mailto:sammy.a.nabors@nasa.gov). Refer to MFS-32584-1.*

## Dielectric Covered Planar Antennas at Submillimeter Wavelengths for Terahertz Imaging

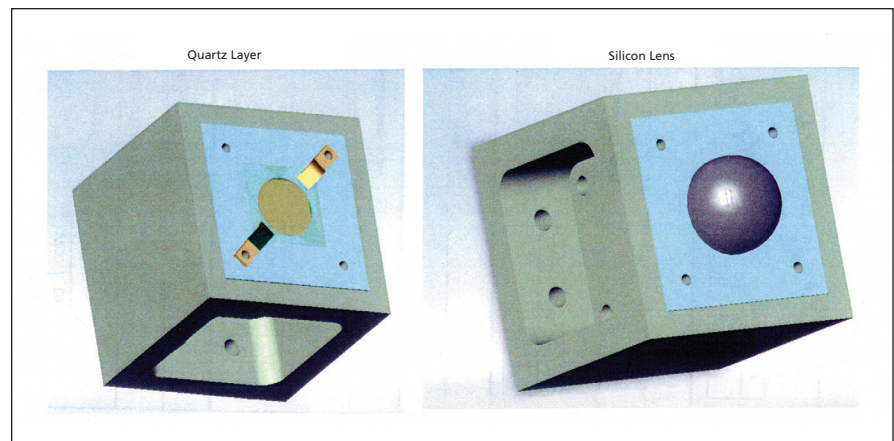
**This technology has potential uses for terahertz radar imagers, radiometers, and spectrometers for earth-science observing instruments.**

NASA's Jet Propulsion Laboratory, Pasadena, California

Most optical systems require antennas with directive patterns. This means that the physical area of the antenna will be large in terms of the wavelength. When non-cooled systems are used, the losses of microstrip or coplanar waveguide lines impede the use of standard patch or slot antennas for a large number of elements in a phased array format.

Traditionally, this problem has been solved by using silicon lenses. However, if an array of such highly directive antennas is to be used for imaging applications, the fabrication of many closely spaced lenses becomes a problem. Moreover, planar antennas are usually fed by microstrip or coplanar waveguides while the mixer or the detector elements (usually Schottky diodes) are coupled in a waveguide environment. The coupling between the antenna and the detector/mixer can be a fabrication challenge in an imaging array at submillimeter wavelengths.

Antennas excited by a waveguide (TE<sub>10</sub>) mode makes use of dielectric superlayers to increase the directivity. These antennas create a kind of Fabry-Perot cavity between the ground plane and the first layer of dielectric. In reality, the antenna operates as a leaky wave mode where a leaky wave pole propagates along the cavity while it radiates. Thanks to this pole, the directivity of a



The Waveguide Block with the quartz layer (left) and the silicon lens (right).

small antenna is considerably enhanced.

The antenna consists of a waveguide feed, which can be coupled to a mixer or detector such as a Schottky diode via a standard probe design. The waveguide is loaded with a double-slot iris to perform an impedance match and to suppress undesired modes that can propagate on the cavity. On top of the slot there is an air cavity and on top, a small portion of a hemispherical lens. The fractional bandwidth of such antennas is around 10 percent, which is good enough for heterodyne imaging applications.

The new geometry makes use of a sili-

con lens instead of dielectric quarter wavelength substrates. This design presents several advantages when used in the submillimeter-wave and terahertz bands:

- Antenna fabrication compatible with lithographic techniques.
- Much simpler fabrication of the lens.
- A simple quarter-wavelength matching layer of the lens will be more efficient if a smaller portion of the lens is used.
- The directivity is given by the lens diameter instead of the leaky pole (the bandwidth will not depend anymore on the directivity but just on the initial cavity).

The feed is a standard waveguide, which

is compatible with proven Schottky diode mixer/detector technologies.

The development of such technology will benefit applications where submillimeter-wave heterodyne array designs are required. The main fields are national security, planetary exploration, and biomedicine. For national security, wideband submillimeter radars could be an effective tool for the standoff detection of hidden weapons or bombs concealed by clothing or packaging. In the field of planetary exploration, wideband

submillimeter radars can be used as a spectrometer to detect trace concentrations of chemicals in atmospheres that are too cold to rely on thermal imaging techniques. In biomedicine, an imaging heterodyne system could be helpful in detecting skin diseases.

*This work was done by Goutam Chattopadhyay, John J. Gill, Anders Skalare, Choonsup Lee, and Nuria Llombart, and Peter H. Siegel of Caltech for NASA's Jet Propulsion Laboratory. Further information is contained in a TSP (see page 1).*

*In accordance with Public Law 96-517, the contractor has elected to retain title to this invention. Inquiries concerning rights for its commercial use should be addressed to:*

*Innovative Technology Assets Management  
JPL*

*Mail Stop 202-233  
4800 Oak Grove Drive  
Pasadena, CA 91109-8099*

*E-mail: iaoffice@jpl.nasa.gov*

*Refer to NPO-46969, volume and number of this NASA Tech Briefs issue, and the page number.*

---

## Automated Cryocooler Monitor and Control System

**Small-scale cryogenic cooler applications include medical imaging for MRI systems and infrared sensor cooling.**

*NASA's Jet Propulsion Laboratory, Pasadena, California*

A system was designed to automate cryogenically cooled low-noise amplifier systems used in the NASA Deep Space Network. It automates the entire operation of the system including cool-down, warm-up, and performance monitoring. The system is based on a single-board computer with custom software and hardware to monitor and control the cryogenic operation of the system. The system provides local display and control, and can be operated remotely via a Web interface.

The system controller is based on a commercial single-board computer with onboard data acquisition capability. The commercial hardware includes a microprocessor, an LCD (liquid crystal display), seven LED (light emitting diode) displays, a seven-key keypad, an Ethernet interface, 40 digital I/O (input/output) ports, 11 A/D (analog to digital) inputs, four D/A (digital to analog) outputs,

and an external relay board to control the high-current devices.

The temperature sensors used are commercial silicon diode devices that provide a non-linear voltage output proportional to temperature. The devices are excited with a 10-microamp bias current. The system is capable of monitoring and displaying three temperatures.

The vacuum sensors are commercial thermistor devices. The output of the sensors is a non-linear voltage proportional to vacuum pressure in the 1-Torr to 1-millitorr range. Two sensors are used. One measures the vacuum pressure in the cryocooler and the other the pressure at the input to the vacuum pump. The helium pressure sensor is a commercial device that provides a linear voltage output from 1 to 5 volts, corresponding to a gas pressure from 0 to 3.5 MPa ( $\approx 500$  psig).

Control of the vacuum process is accomplished with a commercial electrically

operated solenoid valve. A commercial motor starter is used to control the input power of the compressor. The warm-up heaters are commercial power resistors sized to provide the appropriate power for the thermal mass of the particular system, and typically provide 50 watts of heat.

There are four basic operating modes. "Cool" mode commands the system to cool to normal operating temperature. "Heat" mode is used to warm the device to a set temperature near room temperature. "Pump" mode is a maintenance function that allows the vacuum system to be operated alone to remove accumulated contaminants from the vacuum area. In "Off" mode, no power is applied to the system.

*This work was done by Michael J. Britcliffe, Theodore R. Hanson, and Larry E. Fowler of Caltech for NASA's Jet Propulsion Laboratory. Further information is contained in a TSP (see page 1). NPO-47246*

---

## Broadband Achromatic Phase Shifter for a Nulling Interferometer

**A uniform broadband phase shift is achieved while minimizing intensity, polarization, and chromatic spread differences between interferometer beams.**

*Goddard Space Flight Center, Greenbelt, Maryland*

Nulling interferometry is a technique for imaging exoplanets in which light from the parent star is suppressed using destructive interference. Light from the star is divided into two beams and a phase shift of  $\pi$  radians is introduced into one of the beams. When the beams are recombined, they destructively in-

terfere to produce a deep null. For monochromatic light, this is implemented by introducing an optical path difference (OPD) between the two beams equal to  $\lambda/2$ , where  $\lambda$  is the wavelength of the light. For broadband light, however, a different phase shift will be introduced at each wavelength and the

two beams will not effectively null when recombined.

Various techniques have been devised to introduce an achromatic phase shift — a phase shift that is uniform across a particular bandwidth. One popular technique is to use a series of dispersive elements to introduce a wavelength-de-

pendent optical path in one or both of the arms of the interferometer. By intelligently choosing the number, material and thickness of a series of glass plates, a nearly uniform, arbitrary phase shift can be introduced between two arms of an interferometer.

There are several constraints that make choosing the number, type, and thickness of materials a difficult problem, such as the size of the bandwidth to be nulled. Several solutions have been found for bandwidths on the order of 20 to 30 percent ( $\Delta\lambda/\lambda_c$ ) in the mid-infrared region. However, uniform phase shifts over a larger bandwidth in the visible regime between 480 to 960 nm (67 percent) remain difficult to obtain at the tolerances necessary for exoplanet detection.

A configuration of 10 dispersive glass plates was developed to be used as an achromatic phase shifter in nulling interferometry. Five glass plates were placed in each arm of the interferometer and an additional vacuum distance was also included in the second arm of

the interferometer. This configuration creates a phase shift of  $\pi$  radians with an average error of  $5.97 \times 10^{-8}$  radians and standard deviation of  $3.07 \times 10^{-4}$  radians. To reduce ghost reflections and interference effects from neighboring elements, the glass plates are tilted such that the beam does not strike each plate at normal incidence. Reflections will therefore walk out of the system and not contribute to the intensity when the beams are recombined.

Tilting the glass plates, however, introduces several other problems that must be mitigated: (1) the polarization of a beam changes when refracted at an interface at non-normal incidence; (2) the beam experiences lateral chromatic spread as it traverses multiple glass plates; (3) at each surface, wavelength-dependent intensity losses will occur due to reflection. For a fixed angle of incidence, each of these effects must be balanced between each arm of the interferometer in order to ensure a deep null.

The solution was found using a nonlinear optimization routine that minimized an objective function relating phase shift, intensity difference, chromatic beam spread, and polarization difference to the desired parameters: glass plate material and thickness. In addition to providing a uniform, broadband phase shift, the configuration achieves an average difference in intensity transmission between the two arms of the interferometer of 0.016 percent with a standard deviation of  $3.64 \times 10^{-4}$  percent, an average difference in polarization between the two arms of the interferometer of  $5.47 \times 10^{-5}$  percent with a standard deviation of  $1.57 \times 10^{-6}$  percent, and an average chromatic beam shift between the two arms of the interferometer of  $-47.53$  microns with a wavelength-by-wavelength spread of 0.389 microns.

*This work was done by Matthew R. Bolcar and Richard G. Lyon of Goddard Space Flight Center. Further information is contained in a TSP (see page 1). GSC-15830-1*

---

## Super Dwarf Wheat for Growth in Confined Spaces

*Lyndon B. Johnson Space Center, Houston, Texas*

USU-Perigee is a dwarf red spring wheat that is a hybrid of a high-yield early tall wheat (USU-Apogee) and a low-yield, extremely short wheat that has poor agronomic characteristics. USU-Perigee was selected for its extremely short height ( $\approx 0.3$  m) and high yield — characteristics that make it suitable for growth in confined spaces in controlled environments. Other desirable characteristics include rapid development and resistance to a

leaf-tip necrosis, associated with calcium deficiency, that occurs in other wheat cultivars under rapid-growth conditions (particularly, continuous light).

Heads emerge after only 21 days of growth in continuous light at a constant temperature of 25 °C. In tests, USU-Perigee was found to outyield other full dwarf (defined as  $< 0.4$  m tall) wheat cultivars: The yield advantage at a constant temperature of 23 °C was found to be

about 30 percent. Originally intended as a candidate food crop to be grown aboard spacecraft on long missions, this cultivar could also be grown in terrestrial growth chambers and could be useful for plant-physiology and -pathology studies.

*This work was done by Bruce Bugbee of Utah State University for Johnson Space Center. For more information, see [www.usu.edu/cpl/Progression.pdf](http://www.usu.edu/cpl/Progression.pdf). MSC-24200-1*

---

## Fine Guidance Sensing for Coronagraphic Observatories

*NASA's Jet Propulsion Laboratory, Pasadena, California*

Three options have been developed for Fine Guidance Sensing (FGS) for coronagraphic observatories using a Fine Guidance Camera within a coronagraphic instrument. Coronagraphic observatories require very fine precision pointing in order to image faint objects at very small distances from a target star. The Fine Guidance Camera measures the direction to the target star.

The first option, referred to as Spot, was to collect all of the light reflected from a coronagraph occulter onto a focal plane, producing an Airy-type point spread function (PSF). This would allow almost all of the starlight from the central star to be used for centroiding. The second approach, referred to as Punctured Disk, collects the light that bypasses a central obscuration, producing a PSF with a punctured

central disk. The final approach, referred to as Lyot, collects light after passing through the occulter at the Lyot stop.

The study includes generation of representative images for each option by the science team, followed by an engineering evaluation of a centroiding or a photometric algorithm for each option. After the alignment of the coronagraph to the fine guidance sys-

tem, a “nulling” point on the FGS focal point is determined by calibration. This alignment is implemented by a fine alignment mechanism that is part of the fine guidance camera selection

mirror. If the star images meet the modeling assumptions, and the star “centroid” can be driven to that nulling point, the contrast for the coronagraph will be maximized.

*This work was done by Paul Brugarolas, James W. Alexander, John T. Trauger, and Dwight C. Moody of Caltech for NASA’s Jet Propulsion Laboratory. For more information, contact [iaoffice@jpl.nasa.gov](mailto:iaoffice@jpl.nasa.gov). NPO-47067*

---

## Single-Antenna Temperature- and Humidity-Sounding Microwave Receiver

**This technology has applications in imagers and broadband communications.**

*NASA’s Jet Propulsion Laboratory, Pasadena, California*

For humidity and temperature sounding of Earth’s atmosphere, a single-antenna/LNA (low-noise amplifier) is needed in place of two separate antennas for the two frequency bands. This results in significant mass and power savings for GeoSTAR that is comprised of hundreds of antennas per frequency channel. Furthermore, spatial anti-aliasing would reduce the number of horns. An anti-aliasing horn antenna will enable focusing the instrument field of view to the “hurricane corridor” by reducing spatial aliasing, and thus reduce the number of required horns by up to 50 percent.

The single antenna/receiver assembly was designed and fabricated by a commercial vendor. The 118–183-GHz

horn is based upon a profiled, smooth-wall design, and the OMT (orthomode transducer) on a quad-ridge design. At the input end, the OMT presents four very closely spaced ridges [0.0007 in. (18  $\mu$ m)]. The fabricated assembly contains a single horn antenna and low-noise broadband receiver front-end assembly for passive remote sensing of both temperature and humidity profiles in the Earth’s atmosphere at 118 and 183 GHz. The wideband feed with dual polarization capability is the first broadband low noise MMIC receiver with the 118 to 183 GHz bandwidth.

This technology will significantly reduce PATH/GeoSTAR mass and power

while maintaining 90 percent of the measurement capabilities. This is required for a Mission-of-Opportunity on NOAA’s GOES-R satellite now being developed, which in turn will make it possible to implement a Decadal-Survey mission for a fraction of the cost and much sooner than would otherwise be possible.

*This work was done by Daniel J. Hoppe, David M. Pukala, Bjorn H. Lambrigtsen, Mary M. Soria, Heather R. Owen, Alan B. Tanner, Peter J. Bruneau, Alan K. Johnson, Pekka P. Kangaslahti, and Todd C. Gaier of Caltech for NASA’s Jet Propulsion Laboratory. Further information is contained in a TSP (see page 1). NPO-47351*

---

## Multi-Wavelength, Multi-Beam, and Polarization-Sensitive Laser Transmitter for Surface Mapping

**This laser transmitter can be used for precision mapping and remote sensing.**

*Goddard Space Flight Center, Greenbelt, Maryland*

A multi-beam, multi-color, polarized laser transmitter has been developed for mapping applications. It uses commercial off-the-shelf components for a low-cost approach for a ruggedized laser suitable for field deployment.

The laser transmitter design is capable of delivering dual wavelengths, multiple beams on each wavelength with equal (or variable) intensities per beam, and a well-defined state of polarization. This laser transmitter has been flown on several airborne campaigns for the Slope Imaging Multi-Polarization Photon Counting Lidar (SIMPL) instrument, and at the time of this reporting is at a technology readiness level of between 5 and 6.

The laser is a 1,064-nm microchip high-repetition-rate laser emitting en-

ergy of about 8 microjoules per pulse. The beam was frequency-doubled to 532 nm using a KTP (KTiOPO<sub>4</sub>) nonlinear crystal [other nonlinear crystals such as LBO (LiB<sub>3</sub>O<sub>5</sub>) or periodically poled lithium niobate can be used as well, depending on the conversion efficiency requirements], and the conversion efficiency was approximately 30 percent. The KTP was under temperature control using a thermoelectric cooler and a feedback monitoring thermistor. The dual-wavelength beams were then spectrally separated and each color went through its own optical path, which consisted of a beam-shaping lens, quarter-wave plate (QWP), and a birefringent crystal (in this case, a calcite crystal, but others such as vanadate can be used).

The QWP and calcite crystal set was used to convert the laser beams from a linearly polarized state to circularly polarized light, which when injected into a calcite crystal, will spatially separate the circularly polarized light into the two linear polarized components. The spatial separation of the two linearly polarized components is determined by the length of the crystal. A second set of QWP and calcite then further separated the two beams into four. Additional sets of QWP and calcite can be used to further split the beams into multiple orders of two.

The spatially separated beams had alternating linearly polarization states; a half-wave plate (HWP) array was then made to rotate the alternating states of

polarization (SOP) so that all of the beams would have the same SOP. The two wavelength beam paths were then recombined using a dichroic filter such that they were co-aligned. A neg-

ative lens array following the HWP array was used to provide specific beam divergence. A final lens was used to provide the angular spread of the multiple beamlets.

*This work was done by Anthony W. Yu, Luis Ramos-Izquierdo, David Harding, and Tim Huss of Goddard Space Flight Center. Further information is contained in a TSP (see page 1). GSC-15950-1*

---

## **Optical Communications Link to Airborne Transceiver**

*NASA's Jet Propulsion Laboratory, Pasadena, California*

An optical link from Earth to an aircraft demonstrates the ability to establish a link from a ground platform to a transceiver moving overhead. An airplane has a challenging disturbance environment including airframe vibrations and occasional abrupt changes in attitude during flight. These disturbances make it difficult to maintain pointing lock in an optical transceiver in an airplane. Acquisition can also be challenging. In the case of the aircraft link, the ground station initially has no precise knowledge of the aircraft's location.

An airborne pointing system has been designed, built, and demonstrated using direct-drive brushless DC motors for passive isolation of pointing disturbances and for high-bandwidth control feedback. The airborne transceiver uses a GPS-INS system to determine the aircraft's position and attitude, and to then illuminate the ground station initially for acquisition.

The ground transceiver participates in link-pointing acquisition by first using a wide-field camera to detect initial illumination from the airborne bea-

con, and to perform coarse pointing. It then transfers control to a high-precision pointing detector. Using this scheme, live video was successfully streamed from the ground to the aircraft at 270 Mb/s while simultaneously downlinking a 50 kb/s data stream from the aircraft to the ground.

*This work was done by Martin W. Regehr, Joseph M. Kovalik, and Abhijit Biswas of Caltech for NASA's Jet Propulsion Laboratory. For more information, contact [iaoffice@jpl.nasa.gov](mailto:iaoffice@jpl.nasa.gov). NPO-47181*



## Ascent Heating Thermal Analysis on Spacecraft Adaptor Fairings

*John H. Glenn Research Center, Cleveland, Ohio*

When the Crew Exploration Vehicle (CEV) is launched, the spacecraft adaptor (SA) fairings that cover the CEV service module (SM) are exposed to aero heating. Thermal analysis is performed to compute the fairing temperatures and to investigate whether the temperatures are within the material limits for nominal ascent aero-heating case. The ascent heating is analyzed by using computational fluid dynamics (CFD) and engineering codes at Marshall Space Flight Center. The aero-heating environment data used for this work is known as Thermal Environment 3 (TE3) heating data. One of the major concerns is with the SA fairings covering the CEV SM and the SM/crew launch vehicle (CLV) flange interface. The TE3 heating

rate is a function of time, wall temperature, and the spatial locations. The implementation of the TE3 heating rate as boundary conditions in the thermal analysis becomes challenging.

The ascent heating thermal analysis on SA fairings and SM/CLV flange interface are performed using two commercial software packages: Cullimore & Ring (C&R) Thermal Desktop (TD) 5.1 and MSC Patran 2007r1 b. TD is the pre- and post-processor for SINDA, which is a finite-difference-based solver. In TD, the geometry is built and meshed, the boundary conditions are defined, and then SINDA is used to compute temperatures. MSC Pthermal is a finite-element-based thermal solver. MSC Patran

is the pre- and post-processor for Pthermal. Regarding the boundary conditions, the convection, contact resistance, and heat load can be imposed in different ways in both programs. These two software packages are used to build the thermal model for the same analysis to validate each other and show the differences in the modeling details.

*This work was done by Xiao Yen Wang, James Yuko, and Brian Motil of Glenn Research Center.*

*Inquiries concerning rights for the commercial use of this invention should be addressed to NASA Glenn Research Center, Innovative Partnerships Office, Attn: Steve Fedor, Mail Stop 4-8, 21000 Brookpark Road, Cleveland, Ohio 44135. Refer to LEW-18471-1.*

## Entanglement in Self-Supervised Dynamics

*NASA's Jet Propulsion Laboratory, Pasadena, California*

A new type of correlation has been developed similar to quantum entanglement in self-supervised dynamics (SSD). SSDs have been introduced as a quantum-classical hybrid based upon the Madelung equation in which the quantum potential is replaced by an information potential. As a result, SSD

preserves the quantum topology along with superposition, entanglement, and wave-particle duality. At the same time, it can be implemented in any scale including the Newtonian scale. The main properties of SSD associated with simulating intelligence have been formulated. The attention with this innova-

tion is focused on intelligent agents' interaction based upon the new fundamental non-Newtonian effect; namely, entanglement.

*This work was done by Michail Zak of Caltech for NASA's Jet Propulsion Laboratory. For more information, contact [iaoffice@jpl.nasa.gov](mailto:iaoffice@jpl.nasa.gov). NPO-47493*

## Prioritized LT Codes

**These forward erasure correcting codes apply proper matching of data priority and data redundancy to protect against packet drops in image, voice, and video transmissions where not all bits are created equal.**

*NASA's Jet Propulsion Laboratory, Pasadena, California*

The original Luby Transform (LT) coding scheme is extended to account for data transmissions where some information symbols in a message block are more important than others. Prioritized LT codes provide unequal error protection (UEP) of data on an erasure channel by modifying the original LT encoder. The prioritized algorithm improves high-priority data protection

without penalizing low-priority data recovery. Moreover, low-latency decoding is also obtained for high-priority data due to fast encoding. Prioritized LT codes only require a slight change in the original encoding algorithm, and no changes at all at the decoder. Hence, with a small complexity increase in the LT encoder, an improved UEP and low-decoding latency performance for high-

priority data can be achieved.

LT encoding partitions a data stream into fixed-sized message blocks each with a constant number of information symbols. To generate a code symbol from the information symbols in a message, the Robust-Soliton probability distribution is first applied in order to determine the number of information symbols to be used to compute the code symbol. Then,

the specific information symbols are chosen uniform randomly from the message block. Finally, the selected information symbols are XORed to form the code symbol. The Prioritized LT code construction includes an additional restriction that code symbols formed by a relatively small number of XORed information symbols select some of these information symbols from the pool of high-priority data. Once high-priority data are fully covered, encoding continues with the conventional LT approach where code symbols are generated by selecting information symbols from the entire message block including all different priorities. Therefore, if code symbols de-

rived from high-priority data experience an unusual high number of erasures, Prioritized LT codes can still reliably recover both high- and low-priority data. This hybrid approach decides not only “how to encode” but also “what to encode” to achieve UEP. Another advantage of the priority encoding process is that the majority of high-priority data can be decoded sooner since only a small number of code symbols are required to reconstruct high-priority data. This approach increases the likelihood that high-priority data is decoded first over low-priority data.

The Prioritized LT code scheme achieves an improvement in high-prior-

ity data decoding performance as well as overall information recovery without penalizing the decoding of low-priority data, assuming high-priority data is no more than half of a message block. The cost is in the additional complexity required in the encoder. If extra computation resource is available at the transmitter, image, voice, and video transmission quality in terrestrial and space communications can benefit from accurate use of redundancy in protecting data with varying priorities.

*This work was done by Simon S. Woo and Michael K. Cheng of Caltech for NASA's Jet Propulsion Laboratory. For more information, contact iaoffice@jpl.nasa.gov. NPO-46653*

---

## ➤ Fast Image Texture Classification Using Decision Trees

**The algorithms used can be applied to robotics, image retrieval for Web searching, and computer vision for electronic devices.**

*NASA's Jet Propulsion Laboratory, Pasadena, California*

Texture analysis would permit improved autonomous, onboard science data interpretation for adaptive navigation, sampling, and downlink decisions. These analyses would assist with terrain analysis and instrument placement in both macroscopic and microscopic image data products. Unfortunately, most state-of-the-art texture analysis demands computationally expensive convolutions of filters involving many floating-point operations. This makes them infeasible for radiation-hardened computers and space-flight hardware.

A new method approximates traditional texture classification of each image pixel with a fast decision-tree

classifier. The classifier uses image features derived from simple filtering operations involving integer arithmetic. The texture analysis method is therefore amenable to implementation on FPGA (field-programmable gate array) hardware.

Image features based on the “integral image” transform produce descriptive and efficient texture descriptors. Training the decision tree on a set of training data yields a classification scheme that produces reasonable approximations of optimal “texton” analysis at a fraction of the computational cost. A decision-tree learning algorithm employing the traditional k-means criterion of inter-cluster variance is used to learn tree structure

from training data. The result is an efficient and accurate summary of surface morphology in images.

This work is an evolutionary advance that unites several previous algorithms (k-means clustering, integral images, decision trees) and applies them to a new problem domain (morphology analysis for autonomous science during remote exploration). Advantages include order-of-magnitude improvements in runtime, feasibility for FPGA hardware, and significant improvements in texture classification accuracy.

*This work was done by David R. Thompson of Caltech for NASA's Jet Propulsion Laboratory. For more information, contact iaoffice@jpl.nasa.gov. NPO-46548*

---

## ➤ Constraint Embedding Technique for Multibody System Dynamics

**This approach is applicable to multibody dynamics modeling of vehicles and robots.**

*NASA's Jet Propulsion Laboratory, Pasadena, California*

Multibody dynamics play a critical role in simulation testbeds for space missions. There has been a considerable interest in the development of efficient computational algorithms for solving the dynamics of multibody systems. Mass matrix factorization and inversion techniques and the  $O(N)$  class of forward dynamics algorithms developed using a spatial operator algebra stand out as important breakthrough on

this front. Techniques such as these provide the efficient algorithms and methods for the application and implementation of such multibody dynamics models. However, these methods are limited only to tree-topology multibody systems.

Closed-chain topology systems require different techniques that are not as efficient or as broad as those for tree-topology systems. The closed-chain for-

ward dynamics approach consists of treating the closed-chain topology as a tree-topology system subject to additional closure constraints. The resulting forward dynamics solution consists of: (a) ignoring the closure constraints and using the  $O(N)$  algorithm to solve for the “free” unconstrained accelerations for the system; (b) using the tree-topology solution to compute a correction

force to enforce the closure constraints; and (c) correcting the unconstrained accelerations with correction accelerations resulting from the correction forces.

This constraint-embedding technique shows how to use direct embedding to eliminate local closure-loops in the system and effectively convert the system back to a tree-topology system. At this point, standard tree-topology techniques can be brought to bear on the problem. The approach uses a spatial operator algebra approach to formulating the equations of motion. The operators are block-partitioned around the local body subgroups to convert them into aggregate bodies.

Mass matrix operator factorization and inversion techniques are applied to the reformulated tree-topology system. Thus in essence, the new technique allows conversion of a system with closure-constraints into an equivalent tree-topology system, and thus allows one to take advantage of the host of techniques available to the latter class of systems.

This technology is highly suitable for the class of multibody systems where the closure-constraints are local, i.e., where they are confined to small groupings of bodies within the system. Important examples of such local closure-constraints are constraints associated with four-bar

linkages, geared motors, differential suspensions, etc. One can eliminate these closure-constraints and convert the system into a tree-topology system by embedding the constraints directly into the system dynamics and effectively replacing the body groupings with virtual aggregate bodies. Once eliminated, one can apply the well-known results and algorithms for tree-topology systems to solve the dynamics of such closed-chain system.

*This work was done by Abhinandan Jain and Rudranarayan Mukherjee of Caltech for NASA's Jet Propulsion Laboratory. For more information, contact [iaoffice@jpl.nasa.gov](mailto:iaoffice@jpl.nasa.gov). NPO-46950*

---

## ➤ Improved Systematic Pointing Error Model for the DSN Antennas

*NASA's Jet Propulsion Laboratory, Pasadena, California*

New pointing models have been developed for large reflector antennas whose construction is founded on elevation over azimuth mount. At JPL, the new models were applied to the Deep Space Network (DSN) 34-meter antenna's subnet for corrections of their systematic pointing errors; it achieved significant improvement in performance at Ka-band (32-GHz) and X-band (8.4-GHz). The new models provide pointing improvements relative to the traditional models by a factor of two to three, which translate to approximately 3-dB performance improvement at Ka-band. For radio science experiments where blind pointing performance is critical, the new innovation provides a new enabling technology.

The model extends the traditional physical models with higher-order mathematical terms, thereby increasing the resolution of the model for a better fit to the underlying systematic imperfections that are the cause of antenna pointing errors. The philosophy of the traditional model was that all mathematical terms in the model must be traced to a physical phenomenon causing antenna pointing errors. The traditional physical terms are: antenna axis tilts, gravitational flexure, azimuth collimation, azimuth encoder fixed offset, azimuth and elevation skew, elevation encoder fixed offset, residual refraction, azimuth encoder scale error, and antenna pointing de-rotation terms for beam waveguide (BWG) antennas.

Besides the addition of spherical harmonics terms, the new models differ from the traditional ones in that the coefficients for the cross-elevation and elevation corrections are completely independent and may be different, while in the traditional model, some of the terms are identical. In addition, the new software allows for all-sky or mission-specific model development, and can utilize the previously used model as an *a priori* estimate for the development of the updated models.

*This work was done by David J. Rochblatt, Philip M. Withington, and Paul H. Richter of Caltech for NASA's Jet Propulsion Laboratory. For more information, contact [iaoffice@jpl.nasa.gov](mailto:iaoffice@jpl.nasa.gov). NPO-46852*

---

## ➤ Observability and Estimation of Distributed Space Systems via Local Information-Exchange Networks

**An agreement protocol is used as a mechanism for observing formation states from local measurements.**

*NASA's Jet Propulsion Laboratory, Pasadena, California*

Spacecraft formation flying involves the coordination of states among multiple spacecraft through relative sensing, inter-spacecraft communication, and control. Most existing formation-flying estimation algorithms can only be supported via highly centralized, all-to-all, static relative sensing. New algorithms

are proposed that are scalable, modular, and robust to variations in the topology and link characteristics of the formation exchange network. These distributed algorithms rely on a local information exchange network, relaxing the assumptions on existing algorithms.

Distributed space systems rely on a sig-

nal transmission network among multiple spacecraft for their operation. Control and coordination among multiple spacecraft in a formation is facilitated via a network of relative sensing and inter-spacecraft communications. Guidance, navigation, and control rely on the sensing network. This network becomes

more complex the more spacecraft are added, or as mission requirements become more complex.

The observability of a formation state was observed by a set of local observations from a particular node in the formation. Formation observability can be parameterized in terms of the matrices appearing in the formation dynamics and observation matrices. An agreement protocol was used as a mechanism for observing formation states from local measurements. An agreement protocol

is essentially an unforced dynamic system whose trajectory is governed by the interconnection geometry and initial condition of each node, with a goal of reaching a common value of interest. The observability of the interconnected system depends on the geometry of the network, as well as the position of the observer relative to the topology.

For the first time, critical GN&C (guidance, navigation, and control estimation) subsystems are synthesized by bringing the contribution of the space-

craft information-exchange network to the forefront of algorithmic analysis and design. The result is a formation estimation algorithm that is modular and robust to variations in the topology and link properties of the underlying formation network.

*This work was done by Nanaz Fathpour and Fred Y. Hadaegh of Caltech and Mehvan Mesbahi and Amirreza Rahmani of the University of Washington for NASA's Jet Propulsion Laboratory. For more information, contact [iaoffice@jpl.nasa.gov](mailto:iaoffice@jpl.nasa.gov). NPO-46812*

---

## ➤ More-Accurate Model of Flows in Rocket Injectors

*Marshall Space Flight Center, Alabama*

An improved computational model for simulating flows in liquid-propellant injectors in rocket engines has been developed. Models like this one are needed for predicting fluxes of heat in, and performances of, the engines. An important part of predicting performance is predicting fluctuations of temperature, fluctuations of concentrations of chemical species, and effects of turbulence on diffusion of heat and chemical species. Customarily, diffusion effects are represented by parameters known in the art as the Prandtl and Schmidt numbers. Prior formulations include *ad hoc*

assumptions of constant values of these parameters, but these assumptions and, hence, the formulations, are inaccurate for complex flows.

In the improved model, these parameters are neither constant nor specified in advance: instead, they are variables obtained as part of the solution. Consequently, this model represents the effects of turbulence on diffusion of heat and chemical species more accurately than prior formulations do, and may enable more-accurate prediction of mixing and flows of heat in rocket-engine combustion chambers. The model has been

implemented within CRUNCH CFD, a proprietary computational fluid dynamics (CFD) computer program, and has been tested within that program. The model could also be implemented within other CFD programs.

*This work was done by Ashvin Hosangadi, James Chenoweth, Kevin Brinckman, and Sanford Dash of Combustion Research and Flow Technology, Inc. for Marshall Space Flight Center. Inquiries concerning rights for the commercial use of this invention should be addressed to Sammy Nabors, MSFC Commercialization Assistance Lead, at [sammy.a.nabors@nasa.gov](mailto:sammy.a.nabors@nasa.gov). Refer to MFS-32533-1.*

---

## ➤ In-Orbit Instrument-Pointing Calibration Using the Moon as a Target

*NASA's Jet Propulsion Laboratory, Pasadena, California*

A method was developed for in-orbit measurement of the relative pointing of spectrometer channels, and the relationship between the spectrometer channels and the spacecraft coordinate system. In this innovation, individual scans of the Moon, from the three channels, were used to determine the position of the center of the Moon,

with respect to channel-specific coordinates. Comparing the coordinates of the center of the Moon, obtained from individual channels, yields the relative pointing between the channels. Comparing the coordinates of the center of the Moon in one of the channels with the Moon ephemerides and with the spacecraft coordinate measurement,

using the onboard star tracker, yields the relative orientation of the channel optical axes with respect to the spacecraft coordinates.

*This work was done by Alex Abramovici and Harold R. Pollock of Caltech for NASA's Jet Propulsion Laboratory. For more information, contact [iaoffice@jpl.nasa.gov](mailto:iaoffice@jpl.nasa.gov). NPO-47526*



## Books & Reports

### **Reliability of Ceramic Column Grid Array Interconnect Packages Under Extreme Temperatures**

A paper describes advanced ceramic column grid array (CCGA) packaging interconnects technology test objects that were subjected to extreme temperature thermal cycles. CCGA interconnect electronic package printed wiring boards (PWBs) of polyimide were assembled, inspected nondestructively, and, subsequently, subjected to extreme-temperature thermal cycling to assess reliability for future deep-space, short- and long-term, extreme-temperature missions.

The test hardware consisted of two CCGA717 packages with each package divided into four daisy-chained sections, for a total of eight daisy chains to be monitored. The package is 33×33 mm with a 27×27 array of 80%/20% Pb/Sn columns on a 1.27-mm pitch.

The change in resistance of the daisy-chained CCGA interconnects was measured as a function of the increasing number of thermal cycles. Several catastrophic failures were observed after 137 extreme-temperature thermal cycles, as per electrical resistance measurements, and then the tests were continued through 1,058 thermal cycles to corroborate and understand the test results. X-ray and optical inspection have been made after thermal cycling. Optical inspections were also conducted on the CCGA vs. thermal cycles. The optical inspections were conclusive; the x-ray images were not.

Process qualification and assembly is required to optimize the CCGA assembly, which is very clear from the x-rays. Six daisy chains were open out of seven daisy chains, as per experimental test data reported. The daisy chains are open during the cold cycle, and then recover during the hot cycle, though some of them also opened during the hot thermal cycle.

*This work was done by Rajeshuni Ramesham of Caltech for NASA's Jet Propulsion Laboratory. Further information is contained in a TSP (see page 1). NPO-47341*

### **Six Degrees-of-Freedom Ascent Control for Small-Body Touch and Go**

A document discusses a method of controlling touch and go (TAG) of a spacecraft to correct attitude, while ensuring a safe ascent. TAG is a concept whereby a spacecraft is in contact with the surface of a small body, such as a comet or asteroid, for a few seconds or less before ascending to a safe location away from the small body.

The report describes a controller that corrects attitude and ensures that the spacecraft ascends to a safe state as quickly as possible. The approach allocates a certain amount of control authority to attitude control, and uses the rest to accelerate the spacecraft as quickly as possible in the ascent direction. The relative allocation to attitude and position is a parameter whose optimal value is determined using a ground software tool.

This new approach makes use of the full control authority of the spacecraft to cor-

rect the errors imparted by the contact, and ascend as quickly as possible. This is in contrast to prior approaches, which do not optimize the ascent acceleration.

*This work was done by Lars James C. Blackmore of Caltech for NASA's Jet Propulsion Laboratory. Further information is contained in a TSP (see page 1). NPO-47192*

### **Optical-Path-Difference Linear Mechanism for the Panchromatic Fourier Transform Spectrometer**

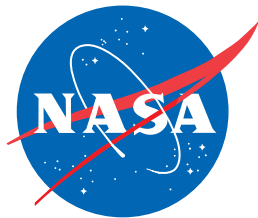
A document discusses a mechanism that uses flex-pivots in a parallelogram arrangement to provide frictionless motion with an unlimited lifetime. A voice-coil actuator drives the parallelogram over the required 5-cm travel. An optical position sensor provides feedback for a servo loop that keeps the velocity within 1 percent of expected value. Residual tip/tilt error is compensated for by a piezo actuator that drives the interferometer mirror.

This mechanism builds on previous work that targeted ground-based measurements. The main novelty aspects include cryogenic and vacuum operation, high reliability for spaceflight, compactness of the design, optical layout compatible with the needs of an imaging FTS (i.e. wide overall field-of-view), and mirror optical coatings to cover very broad wavelength range (i.e., 0.26 to 15  $\mu\text{m}$ ).

*This work was done by Jean-Francois L. Blavier, Matthew C. Heverly, Richard W. Key, and Stanley P. Sander of Caltech for NASA's Jet Propulsion Laboratory. Further information is contained in a TSP (see page 1). NPO-47317*







National Aeronautics and  
Space Administration